Hindawi Publishing Corporation
Advances in Meteorology
Volume 2010, Article ID 284503, 13 pages
doi:10.1155/2010/284503

Research Article

Tropical Atlantic Hurricanes, Easterly Waves, and West African Mesoscale Convective Systems

Yves K. Kouadio,[1,2] Luiz A. T. Machado,[3] and Jacques Servain[4]

[1] *Laboratoire de Physique de l'Atmosphère, University of Cocody, UFR-SSMT, 22 BP 582 Abidjan 22, Cote d'Ivoire*
[2] *CPTEC/INPE, Cachoeira Paulista, SP, Brazil*
[3] *Centro de Previsão de tempo e Estudos Climáticos, Instituto Nacional de Pesquisas Espaciais (CPTEC/INPE), Rodovia Presidente Dutra, km 40, Cachoeira Paulista, SP, Brazil*
[4] *Institut de Recherche pour le Développement (IRD-UR182), Fundação Cearense de Meteorologia e Recursos Hídricos (FUNCEME), Avenida Rui Barbosa 1246, Fortaleza, CE, Brazil*

Correspondence should be addressed to Luiz A. T. Machado, machado@cptec.inpe.br

Received 29 October 2009; Accepted 12 February 2010

Academic Editor: Mladjen Curic

The relationship between tropical Atlantic hurricanes (Hs), atmospheric easterly waves (AEWs), and West African mesoscale convective systems (MCSs) is investigated. It points out atmospheric conditions over West Africa before hurricane formation. The analysis was performed for two periods, June–November in 2004 and 2005, during which 12 hurricanes (seven in 2004, five in 2005) were selected. Using the AEW signature in the 700 hPa vorticity, a backward trajectory was performed to the African coast, starting from the date and position of each hurricane, when and where it was catalogued as a tropical depression. At this step, using the Meteosat-7 satellite dataset, we selected all the MCSs around this time and region, and tracked them from their initiation until their dissipation. This procedure allowed us to relate each of the selected Hs with AEWs and a succession of MCSs that occurred a few times over West Africa before initiation of the hurricane. Finally, a dipole in sea surface temperature (SST) was observed with a positive SST anomaly within the region of H generation and a negative SST anomaly within the Gulf of Guinea. This SST anomaly dipole could contribute to enhance the continental convergence associated with the monsoon that impacts on the West African MCSs formation.

1. Introduction

The tropical North Atlantic is a World Ocean basin where cyclonic activity is intense. It presents a substantial interannual and interdecadal variability [1], depending directly on atmospheric and oceanic conditions. The Atlantic hurricane (H) activity occurs between July and November, and major Hs form in the Main Development Region (MDR), defined as the tropical North Atlantic south of 21°N and the Caribbean Sea. This cyclonic activity mainly originates from the African atmospheric easterly waves (AEWs) that propagate from West Africa towards the tropical North Atlantic basin and the Caribbean Sea [2, 3]. These waves, which have a 3-to-4-day period [4], are responsible for about 60% of tropical storms and minor Hs, and 85% of Hs of strong intensity [5–7]. Several studies [5, 8, 9] have even suggested that some tropical cyclones occurring in the eastern Pacific develop in association with AEWs that were initially generated in Africa and then propagated across the tropical Atlantic and Central America.

Upstream in their propagation across the ocean, these AEWs are themselves generally accompanied by mesoscale convective systems (MCSs), which cross the center Sahel region between 8°N–18°N and 10°W–17°E and dissipate in the tropical Atlantic Ocean towards 20°W [10]. Cotton and Anthes [11] described MCSs as deep convective systems that are considerably larger than individual thunderstorms and are often marked by an extensive middle to upper tropospheric stratiform anvil. Some of these long-lived MCSs can generate midlevel mesoscale vortices, which occur in the stratiform region of the system after the anvil debris has dissipated [12]. In a recent study, Saïdou and Sauvageot

[13] described the cyclogenesis of hurricane Cindy (1999) in the tropical North Atlantic as resulting from a space-time conjunction between MCSs observed off Africa and subsequent easterly wave propagation under warm sea surface conditions.

The goal of this study is to examine atmospheric conditions over West Africa before the initiation of the hurricanes. This study is done by considering the following four elements: the MCSs which initiate over West Africa then dissipate over the ocean, the AEWs which propagate from Africa to the oceanic basin, the surface oceanic conditions in the region of interest, and finally the H occurrences. Our analysis is based on various datasets for the years 2004 and 2005. The original tracking of individual MCSs comprises the core of this study.

The next section presents the dataset used in our analysis. We focus especially on the process developed to access an original database of MCS trajectories. It allows a very precise follow-up, with high-frequency sampling (30 minutes), of each MCS trajectory during its lifespan over continents and the ocean. Research into the association between the onset of a tropical cyclone (which is later classified in the H category) and the West African MCSs embedded in the AEW trajectories represents the midpoint of our analysis. Such events (seven in 2004, five in 2005) were selected and analyzed and are described in the third section. The fourth section describes the abnormal SST conditions which experienced during the same time in the tropical Atlantic. A summary and conclusion are given in the last section.

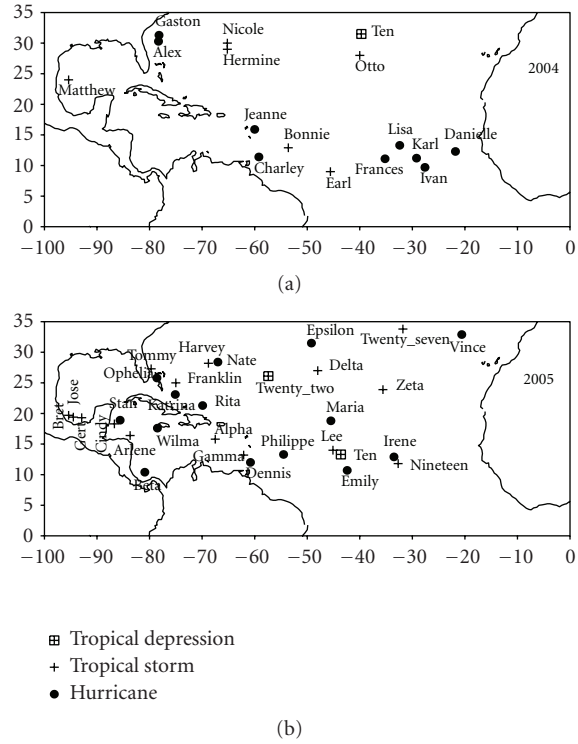

Figure 1: Initiation coordinates of the tropical cyclones observed during 2004 (a) and 2005 (b). Every symbol is related to a tropical cyclone that remained as a tropical depression (TD) or turned into tropical storm (TS) or hurricane (H).

2. Data and Methodology

The tropical cyclone intensity has been prescribed by the National Hurricane Center (NHC) [14]. Three classes are defined according to the Saffir-Simpson hurricane scale [15] from the weakest to the strongest intensity. They relate to the maximum sustained surface wind speed reached during the development stages: tropical depression (TD) with wind speed less than $18\,\mathrm{m\,s^{-1}}$, tropical storm (TS) with wind speed ranged between 18–$33\,\mathrm{m\,s^{-1}}$, and hurricane (H) with wind speed at least $33\,\mathrm{m\,s^{-1}}$. Figure 1 shows the initiation coordinates for the three classes of all tropical cyclones provided by the NHC that were observed during the years 2004 (Figure 1(a)) and 2005 (Figure 1(b)). Let us keep in mind that the initiation coordinates are defined as being the time at which a tropical cyclone is primarily classified as TD.

Sixteen tropical cyclones occurred in 2004: only one remained classified as class TD, six became class TS, and nine reached class H. Among these nine Hs, seven initiated within the band 20°N–10°N: two in the vicinity of the West Indies, and the other five southwest of the Azores Islands, that is, not far from Africa. These last seven Hs are analyzed in this study.

In 2005, there were 31 tropical cyclones, that is, almost twice the number observed in 2004. The repartitioning of these 31 cyclones according to their classes and initiation coordinates is somewhat different from those of the previous year. The tropical cyclones were distributed in the entire Atlantic basin. Despite the large number of tropical cyclones in 2005, fewer hurricanes initiated close to Africa than in 2004. Of the 31 tropical cyclones in 2005, 13 reached the H class (more than 40%), including the dramatic hurricane Katrina, which devastated New Orleans in August (NOAA Magazine, 2005). Of these 13 hurricanes, only five initiated close to Africa, and this subset of five was selected for analysis in this study.

MCSs are largely identified by satellite images [16–20] and by radar over land regions [21]. In this study, we used digital images from the Meteosat-7 satellite over the region 25°N–25°S and 35°W–20°E, from June to November in both 2004 and 2005. This dataset is available in 30-minute time intervals at full spatial resolution ($5\,\mathrm{km} \times 5\,\mathrm{km}$) in the infrared channel. The June–November period largely covers the West African rainy season and the seasonal cyclonic activity in the tropical North Atlantic. Mathon et al. [19] noted that the Meteosat images are useful for cloud system characterization and classification predominantly in West and Central Africa, where the convection is well defined on a very large scale.

Wind fields were extracted from the National Center for Environmental Prediction-National Center for Atmospheric Research (NCEP-NCAR) reanalysis dataset [22] during the same periods of 2004 and 2005. Those data are reported on a $2.5^\circ \times 2.5^\circ$ grid every 6 hours (00:00, 06:00, 12:00, and 18:00 UTC), at 17 pressure levels from 1000 hPa to 10 hPa. Because we focused on the AEWs which are synoptic

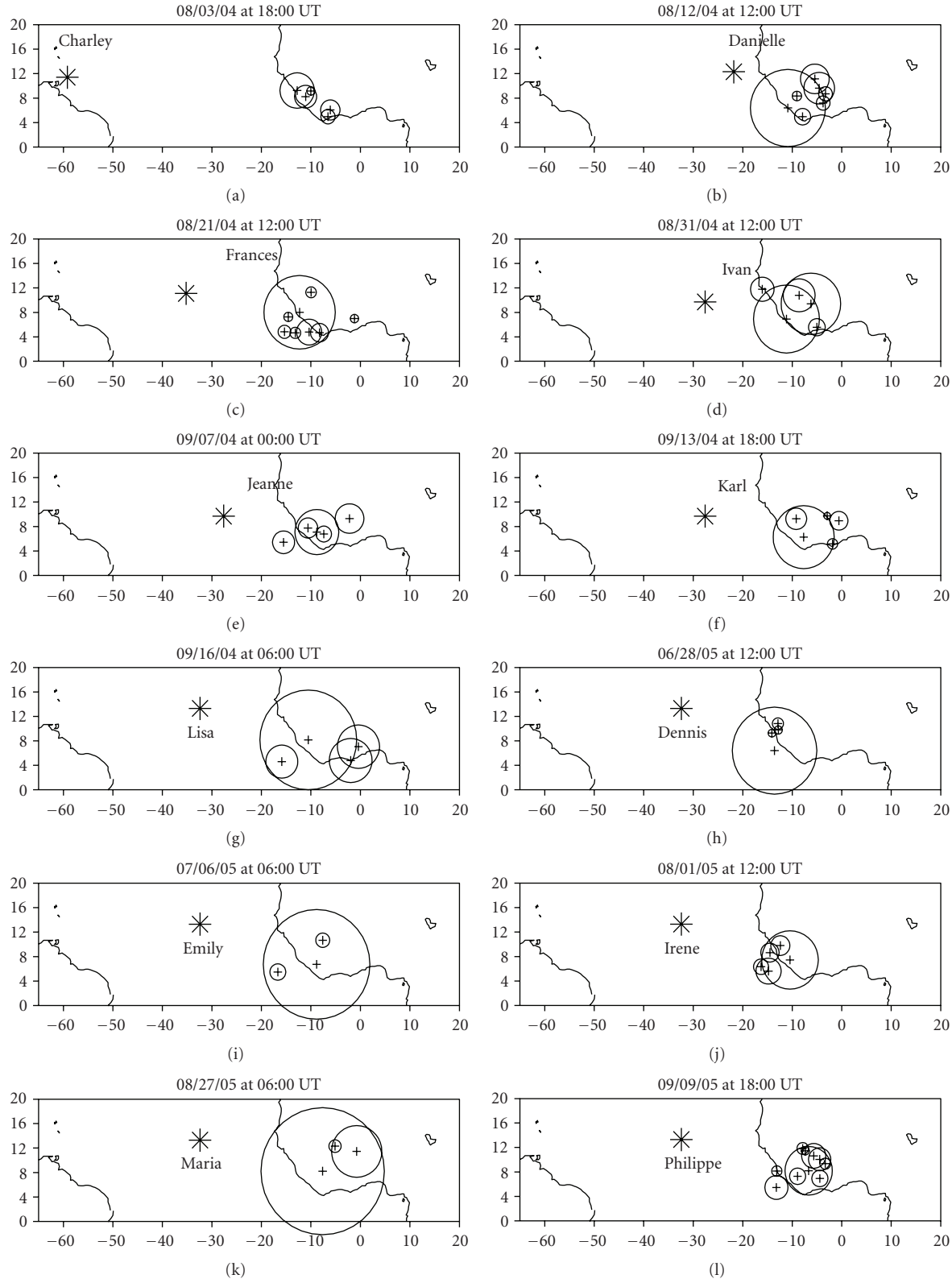

Figure 2: MCSs (>2.5 hours) identified using the backward trajectory of the easterly waves associated with each selected hurricane. The stars mark the coordinates of the initiation positions of the hurricanes. The position (cross) and surface cover (circle) of each MCS are also indicated. The dates indicate when the easterly waves left the West African coast.

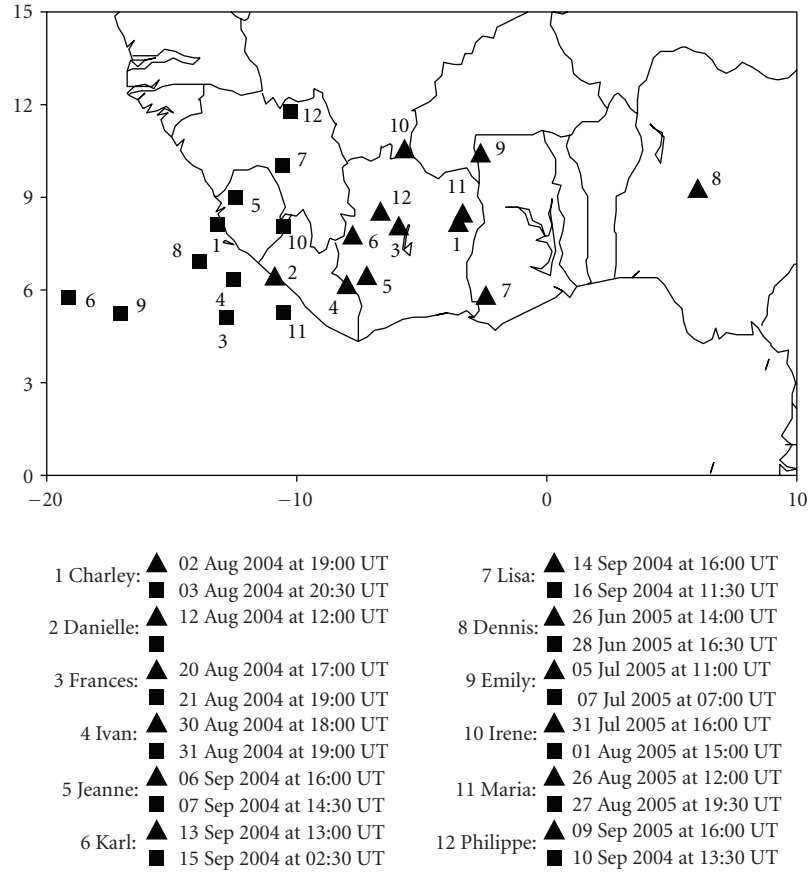

Figure 3: Spatial distribution of the initiation coordinates (triangle) and dissipation coordinates (squares) for the long-lived MCSs (>10 hours) in 2004 and 2005 associated with the 12 selected hurricanes. The split or merged phenomena after the dissipation period are not taken into account. Every number is related to a single event. The first and second dates on the lower panel are related to the initiation and dissipation of the MCSs, respectively. The dissipation of Danielle could not be tracked because of a lack of data.

disturbances that propagate in the North Atlantic and are linked to tropical cyclones, our analyses mainly considered the relative vorticity at 700 hPa [9] deduced from the wind. Daily precipitation data over the ocean were derived from the Global Precipitation Climatology Project—GPCP [23]. The GPCP rainfall is extracted on a $1^\circ \times 1^\circ$ regular grid for the period 2004-2005. This last dataset is deduced from a blending of in situ observations and microwave measurements carried out by various geostationary satellites.

The sea surface conditions were documented for this area in both 2004 and 2005 using Reynolds' weekly SST anomaly [24] extracted from http://iridl.ldeo.columbia.edu/. These data are reported on a $1^\circ \times 1^\circ$ grid.

During their lifespan, MCSs can move, change, grow, shrink, split, or merge into one or more systems. To follow this evolution, it is necessary to track each event in space and time during its lifespan, using a methodology that can be adapted to successive changes in the MCS characteristics. Here, we used a tracking convective cluster model (ForTraCC, Forecasting and Tracking Cloud Cluster), developed and now operational at CPTEC/INPE [25]. The ForTraCC technique, based on the results of former studies [18, 26–29], is an objective method that uses images from geostationary satellites to document the physical characteristics of each individual MCS at each time increment during its lifespan. The main steps of this software are (i) cloud cluster detection based on a threshold of the brightness temperature at the top of the cloud, (ii) evaluation of the morphology and radiative parameters for each MCS detected in the previous step, (iii) space and time tracking for each MCS based on overlapping areas between successive images according to the 30-minute time resolution, and (iv) life-cycle construction and synthetic image generation.

In its basic version [25], ForTraCC uses two fixed threshold temperatures: 235 K to define the whole MCS and 210 K to identify the areas of more intense convection embedded in this MCS. These threshold temperatures have been specified in previous work for Africa [28]. In fact, the characteristics of the MCSs are strongly modulated by the diurnal cycle over the continent and the ocean [26]. For instance, when a fixed threshold is considered, there is an undervaluation of the MCS threshold over the ocean because of the weaker convection. That supposes a loss of information in tracking the MCSs. We thus

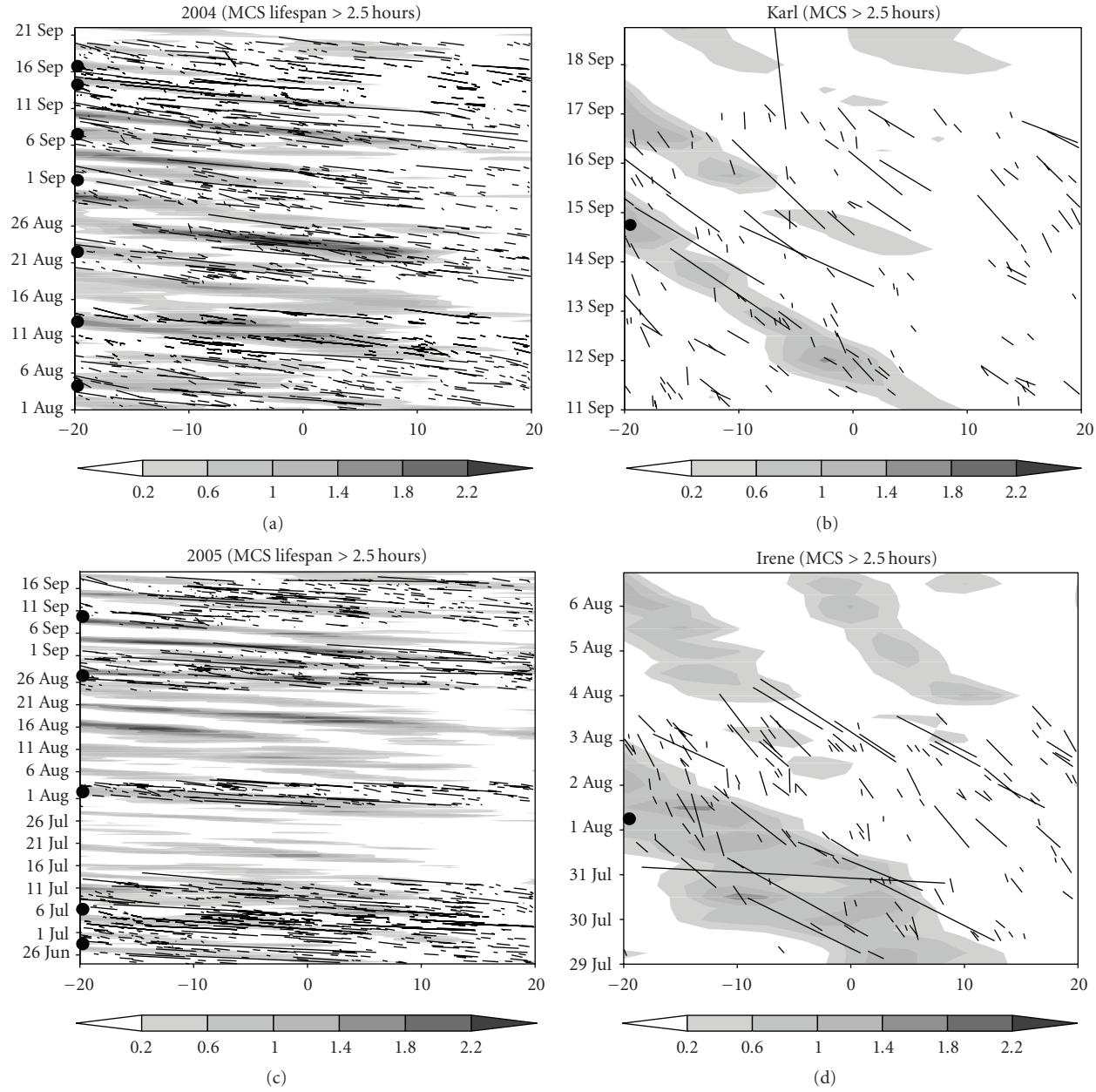

FIGURE 4: ((a) and (c)) The 700 hPa relative vorticity ($\times 10^{-5}$ s^{-1}) in August–September of 2004 (a) and in June–September of 2005 (c) along 20°W–20°E, averaged between 5°N and 15°N. The H initiation coordinates translated up to 20°W are marked as dots. The westward MCS trajectories (>2.5 hours) are only plotted from 20°E to 20°W before the easterly wave left the African coast. ((b) and (d)) Zoom over two different examples: Karl in 2004 (a) and Irene in 2005 (c).

defined a threshold temperature as following the diurnal cycle, according to Morel and Senesi [30], who showed that this method correctly discriminates 80% of MCSs in Europe. This threshold temperature is referred to as the "dynamic threshold", compared with the fixed threshold temperature used in the basic version of ForTraCC. The definition of this dynamic threshold is developed in the appendix.

During the dissipation phase of the MCS, the brightness temperature at the clouds tops increases rapidly. Because of the weaker convection on the ocean, such a system generally fragments into small stratiform clouds, which could persist and propagate westward embedded in one of the numerous easterly wave trajectories. It thus becomes possible to continue to follow the initial perturbation event while analyzing the signature of the associated easterly wave. These waves are generally easily detected from the relative vorticity of the wind field at 700 hPa [31]. Frank [32] noted that there are many easterly waves across the West African coast, although their numbers are apparently not directly related to the numbers of tropical storms.

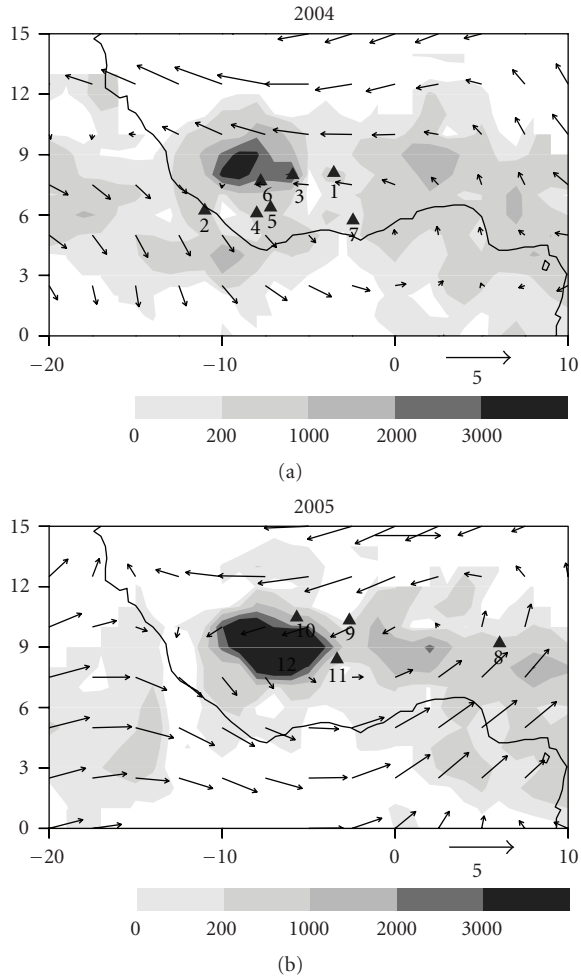

FIGURE 5: Composite cloud coverage ($\times 25\,\text{km}^2$) for the seven events in 2004 (a) and for the five events in 2005 (b). The 700 hPa composite wind vector anomaly calculated from the day when the long-lived MCS is initiated until the day when the easterly wave left the West African coast is also superimposed on the graphics.

3. Results

3.1. MCSs Associated with Hurricane Events. As previously discussed, seven Hs (Charley, Danielle, Frances, Ivan, Jeanne, Karl, and Lisa) that initiated in 2004 within the band 10°N–20°N were selected. Gaston and Alex (see Figure 1(a)), which initiated close to Florida, were considered too distant to be taking account in this study. In 2005, despite the larger number of Hs, only five of them (Dennis, Emily, Irene, Maria, and Philippe), which initiated south of 30°N and east of 60°W (Figure 1(b)), were selected.

Our analysis is directed depending on the two following statements.

(a) Hs that are generated over the eastern and central tropical Atlantic regions are mainly associated with easterly waves propagating from the African continent at an average speed of about $10\,\text{m}\,\text{s}^{-1}$ [4]. These waves initiate during the active hurricane period in July–September, when the midlevel African easterly jet is intensified.

(b) Tracking analysis has shown that most of the MCSs initiate in Africa between 17°W–20°E and 5°N–20°N from June to September. Their great majority dissipates over the continent and does not reach the ocean. Only a few MCSs (~6%) dissipate over the ocean, mostly between the West African coast and 20°W. For reference, we defined the initiation (dissipation) time as being the first (last) available image where the brightness temperature is lesser (greater) than the used threshold at the indicated time.

Considering these two statements, the following procedure was used to study MCSs in Africa a few times before the initiation of the selected Hs. From the date and the geographical location of the initiation of each H, we looked at synchronous and backward easterly wave patterns at a six-hour interval. The 700 hPa unfiltered relative vorticity was used to describe the AEWs. The process was continued backward until these easterly waves "reached" the West African coast (around 17°W). From this position and time, we looked for MCSs that could be associated to the easterly wave perturbation. This search was done at the same time (i.e., within the same six-hour increments), within the limited area around the position at which the easterly wave "reached" the coast. From all the possible concomitant MCSs, we selected only those with lifespan longer than 2.5 hours, and which moved roughly westward, that is, in the direction of the easterly wave previously analyzed. Then, using the ForTraCC technique, we developed a process of backward and forward objective analysis along the MCS trajectories until the dates and positions of their initiation and dissipation were deduced. For the 12 Hs, the selected MCSs nearest the African coast, at the moment of the AEW is leaving the African Coast, are described in Figure 2 by their centers of mass and their areas (represented as circles). We note that for each event, there is one large MCS and many others smaller MCSs in the neighbourhood. These MCSs are usually found around 9°N and 10°W, some of them over the ocean and others over the continent.

The entire process allows the identification of the MCSs. Note that the 12 events of MCSs found by this process are named by the H names. Figure 3 shows the initiation and dissipation positions of the largest and most long-lived (>10 hours lifespan) MCSs among the selected MCSs. The lack of several Meteosat images during the Danielle event (2004) did not allow us to track the MCS until its dissipation. Interestingly, the great majority of MCS initiations occurred inside a relatively limited continental domain around 5°N–11°N, 8°W–2.5°W (i.e., around the Ivory Coast territory). As an exception, the MCS for the Dennis event (June 2005) initiated around 6°E, that is, far east of that region (see Table 1). Moreover, the lifespan of this MCS (87.5 hours) was definitely longer than the average lifespan of all the other events (33 hours). All these MCSs dissipated west of their initiation regions, six over the ocean, one along the African coast, and four over the African continent (note the lack

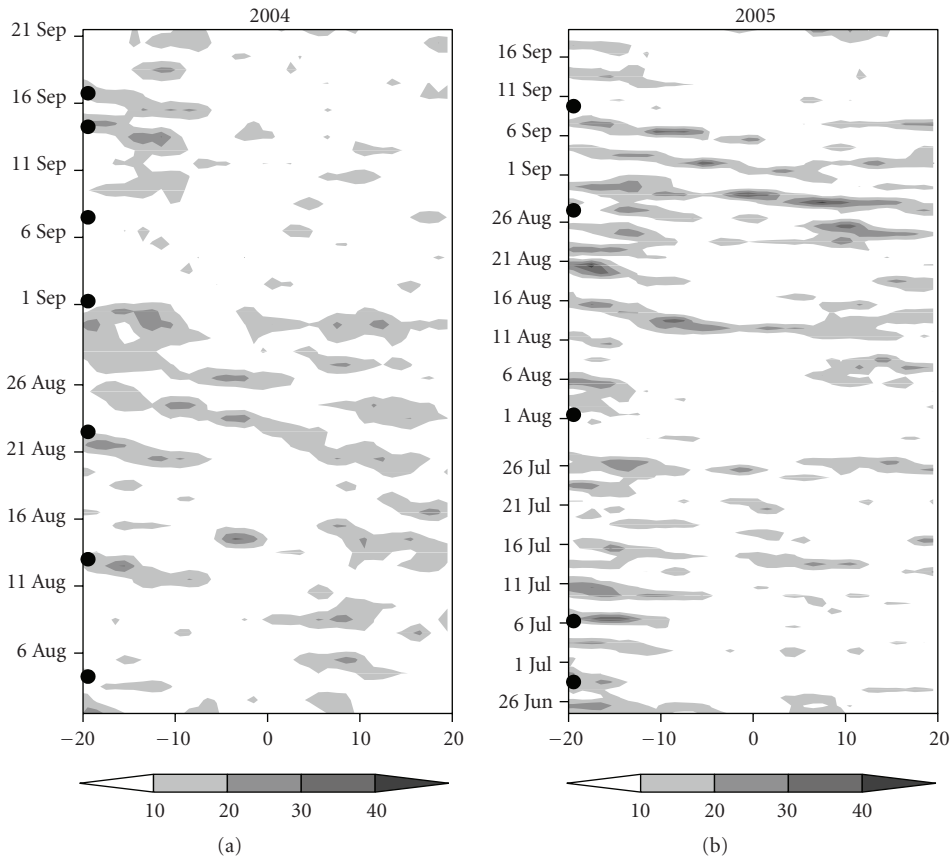

Figure 6: Daily precipitation (mm) along 20°W–20°E in August-September of 2004 (a) and in June–September of 2005 (b), averaged between 5°N and 15°N. The date when AEW for a specific H left the coast of Africa is marked as dot.

of information in the case of Danielle). Lisa and Philippe (numbers 7 and 12 in Figure 3, resp.) are the "most near-continental" events.

Figure 4 shows the Hovmöller space–time diagrams of the 700 hPa unfiltered relative vorticities along 20°W–20°E, averaged between 5°N and 15°N. The 2004 events are at the top and the 2005 events are on the bottom. The dots are a longitudinal translation from the position of each selected H (see Figure 1) up to 20°W. The date when the AEW of a specific H leaves the African coast is also indicated. A zoom is shown on the right for two different examples. The first example (panel at the right top) is related to Karl (2004). The second example (panel at the right bottom) is related to Irene (2005). The easterly waves clearly appear on this figure with similar speeds, close to $10\,\mathrm{m\,s^{-1}}$. The average MCS displacement is also very close to the easterly wave trajectory. Also superimposed on Figure 4 is a selection of the MCS trajectories propagating westward. These MCSs were selected as follows: (i) as already mentioned, MCS tracking was only performed from 20°E to the African coast; (ii) the only MCSs plotted were those that initiated before the date when the AEW associated with a specific H left the African coast; (iii) the panels are representative of MCSs with lifespan greater than 2.5 hours. The MCS displacements embedded in the easterly wave trajectories indicate convective activities between 20°E and the African coast. The MCSs generally had a longer trajectory (longer lifespan) over the continental area (up to 17°W), which is probably explained by the deeper convection over land. Figure 4 shows that many MCS trajectories with different life cycles (including at least one long-lived MCS) followed the AEWs. This succession of MCS families could indicate a regeneration of the fragmented stratiform clouds coming from the dissipation phase of the MCSs (as noted in the previous section) and/or a new birth of MCS.

In the way to study the relationship between the cloud cover produced by the MCSs and the easterly waves, we computed a composite field for 2004 and 2005 MCS-easterly wave coastal cases precedent the Hurricanes events. The cloud coverage was computed for every convective system for 30-minute interval. Winds were computed to the closest time to the NCEP reanalysis as the anomaly for the June-September average of the computed year. The average and anomalies were computed from the date of the initiation of the long-lived MCS (see Figure 3) to the date when the AEW left the African coast (see Figure 2). Figure 5 shows the average of the cloud coverage for the seven events in 2004 (a) and for the five events in 2005 (b). In both 2004 and 2005, the maximum activity of deep convection is observed on average between 8°N and 12°N. This zone corresponds to a region of frequently location of organized convection in West Africa [19]. One can observe the westward flow on the north of 8°N

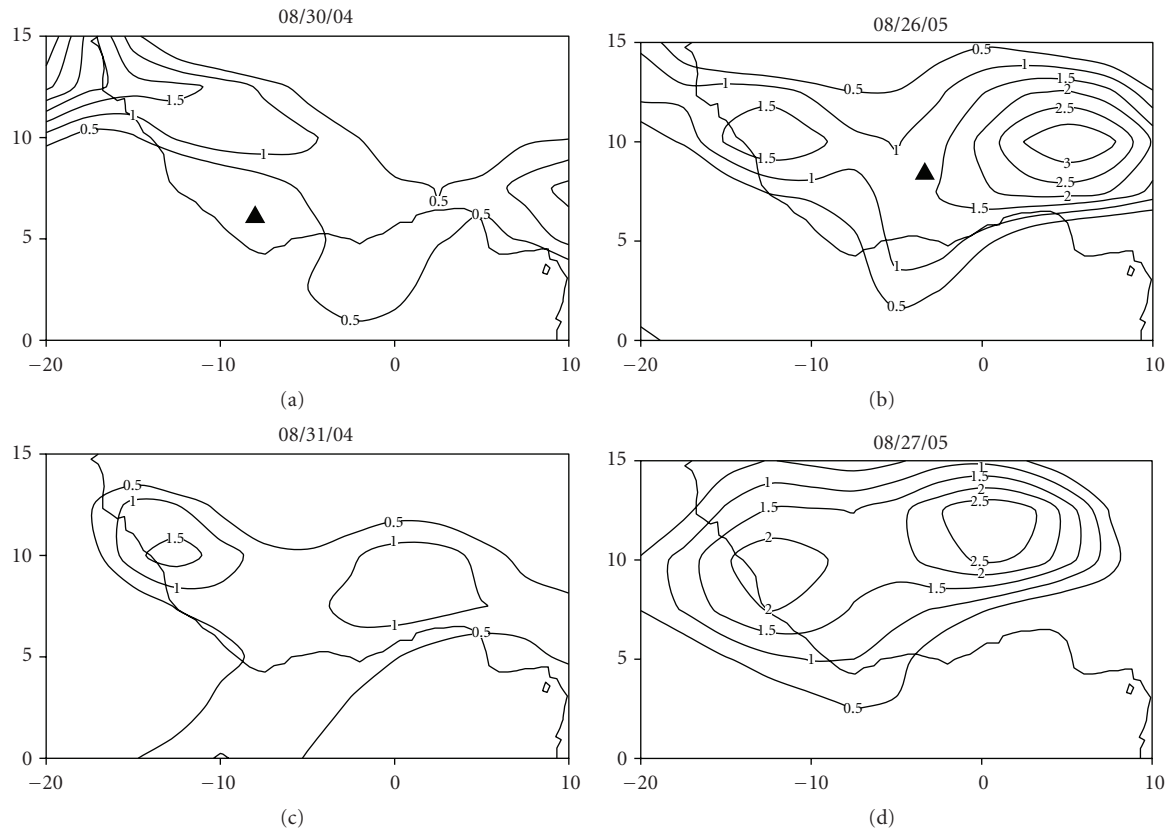

Figure 7: Daily pattern of the 700 hPa unfiltered relative vorticity for the Ivan (left) Maria (right) events, from the day when the long-lived MCS is initiated until the day the easterly wave left the West African coast. Only positive values larger than $0.5 \times 10^{-5}\,s^{-1}$ are plotted. The contour increment is $0.5 \times 10^{-5}\,s^{-1}$. The MCS initiation coordinates are marked as triangles.

showing the presence of the African easterly jet. The easterly wave clearly appears in this pattern, showing a north wind anomalies in the front of the convective core.

Figure 6 illustrates the Hovmöller space–time diagrams for the daily rainfall in both 2004 and 2005 during the same period as shown in Figure 4 (in August to September of 2004 and in June to September of 2005). The precipitation field also shows a discontinuous intensity of the strong rainfall events ($>25\,mm\,day^{-1}$) which is probably a result of the large number of MCSs initiating and dissipating along the easterly wave. This intermittent presence of MCSs illustrates an occurrence of convective activity related to the strong rainfall. The observed rainfall occurrences ($>10\,mm\,day^{-1}$) follow the AEW trajectories and are clearly an example of the association of MCSs and AEWs.

Figure 7 shows two different examples of the daily 700 hPa unfiltered relative vorticity of the day of the initiation of the long-lived MCS and the day when the AEW leaves the African coast. The first example (panels at the left of the figure) is related to Hurricane Ivan, in 2004, which initiated in the eastern basin and the second example (panels at the right of the figure) is related to the Hurricane Maria which initiated in the central basin. Each panel is representative of the 700 hPa vorticity on the day of the largest MCS initiation, and the day when the easterly wave lives the African Coast. In both cases, a westward-moving relative vorticity perturbation was observed from the largest MCS initiation region to the West African coast. The vorticity intensification at the African coast reaches almost $2\,10^{-5}\,s^{-1}$ for the case of Maria and $1.5\,10^{-5}\,s^{-1}$ for the Ivan. Such westward displacement of the vorticity can be associated with the westward advection of the stratiform parts of the convective systems, as suggested by Bartels and Maddox [12]. Thus, one of the possible mechanisms for the intensification of cyclonic vorticity may be the large number of MCSs found embedded within the AEW propagation and the intermittent episodes of dissipation/initiation merging/splitting of the MCS families. This can change the tilting term of the vorticity equation and contributing to the intensification of the easterly wave as suggested by Houze [34].

3.2. Sea Surface Temperature in 2004 and 2005. The thermal condition of the ocean surface is a very important factor in H and MCS formation and for the variability in the relative vorticity [1]. To investigate this feature in our dataset, the SST anomaly fields, derived from the weekly SST 1971–2000 climatology of Reynolds et al. [24], were computed for each of the weeks in 2004 and 2005 that included the initiation dates of the long-lived MCSs for the 12 selected events.

Table 1: Summary information for the 12 selected events in 2004 and 2005 with the long-lived MCSs originating from the African continent. MCS initiation dates and MCS lifespans (hours) are also given. Systems that ended by merging or splitting are considered [33]. The MCS dissipation for Danielle could not be tracked because of a lack of data.

	Hurricane initiations		MCS dissipations			
Name	Date	Coordinates	Date	Coordinates	MCS initiation date	Lifespan (hour)
Charley	08/09/04 12:00 UT	11.4°N; 59.2°W	08/03/04 20:30 UT	8.11°N - 13.16°W	08/02/04 19:00 UT	25.5
Danielle	08/13/04 12:00 UT	12.3°N 21.8°W			08/12/04 12:00 UT	
Frances	08/25/04 00:00 UT	11.1°N; 35.2°W	08/21/04 21:00 UT	5.10°N; 12.82°W	08/20/04 17:00 UT	28
Ivan	09/02/04 18:00 UT	9.7°N; 27.6°W	08/31/04 19:00 UT	6.34°N; 12.52°W	08/30/04 18:00 UT	25
Jeanne	09/13/04 18:00 UT	15.9°N; 60°W	09/07/04 14:30 UT	9°N; 12.46°W	09/06/04 16:00 UT	22.5
Karl	09/16/04 06:00 UT	11.2°N; 29.2°W	09/15/04 02:30 UT	5.75°N; 19.11°W	09/13/2004 13:00 UT	37.5
Lisa	09/19/04 18:00 UT	13.3°N; 32.4°W	09/16/04 11:30 UT	10.03°N; 10.59°W	09/14/04 16:00 UT	43.5
Dennis	07/04/05 18:00 UT	12°N; 60.8°W	06/30/05 05:30 UT	4.44°N; 26.30°W	06/26/05 14:00 UT	87.5
Emily	07/11/05 00:00 UT	10.7°N; 42.4°W	07/07/05 07:00 UT	5.25°N; 17.04°W	07/05/2005 11:00 UT	44
Irene	08/04/05 18:00 UT	12.9°N; 33.5°W	08/02/05 04:30 UT	5.35°N - 10.17°W	07/31/05 16:00 UT	36.5
Maria	09/01/05 12:00 UT	18.8°N; 45.5°W	08/27/05 19:30 UT	5.26°N; 10.51°W	08/26/05 12:00 UT	31.5
Philippe	09/17/05 12:00 UT	13.3°N 54.5°W	09/10/05 13:30 UT	11.79°N; 10.24°W	09/09/05 16:00 UT	26.5

Daily averages of the 1000 hPa wind vectors anomalies were also calculated from the day of the initiation of the long-lived MCS to the day when the AEW left the African coast. Figure 8(a) shows the composite SST for the six different weeks (Karl and Lisa occurred in the same week) and wind anomaly during the seven 2004 events. The same analysis was performed for the five events in 2004 (Figure 8(b)). The initiation coordinates of the selected H are superimposed on the SST anomaly patterns. It is not surprising to note that all the selected Hs were initiated over regions of positive SST anomaly, although not necessarily over their cores. In the 2004 composite, the highest positive SST anomalies (>+1.4°C) were located near the northwest African coast. In the 2005 composite anomaly, two separated cores of positive SST anomaly (>+1.4°C) were positioned along 20°N, one near the African coast and the other centered at 50°W. In the meantime, a wind relaxation was observed up to 5°N (particularly between 10°N and 15°N) in the vicinity of the West African coast during the two years. That relaxation, which was also observed in the mean location of the ITCZ during this period, corresponds not only to an abnormal decrease of the northeast trades but also to an abnormal northern migration of the ITCZ. That could indicate a stronger northern extension of the monsoon, that is, a more important advection of the potential raining on the African Continent.

An interesting point is the negative SST anomaly pattern in the Gulf of Guinea observed in both years, with that of 2005 being mostly 3 times larger (>–0.6°C) than that of 2004 (~–0.2°C). Such negative SST anomaly patterns

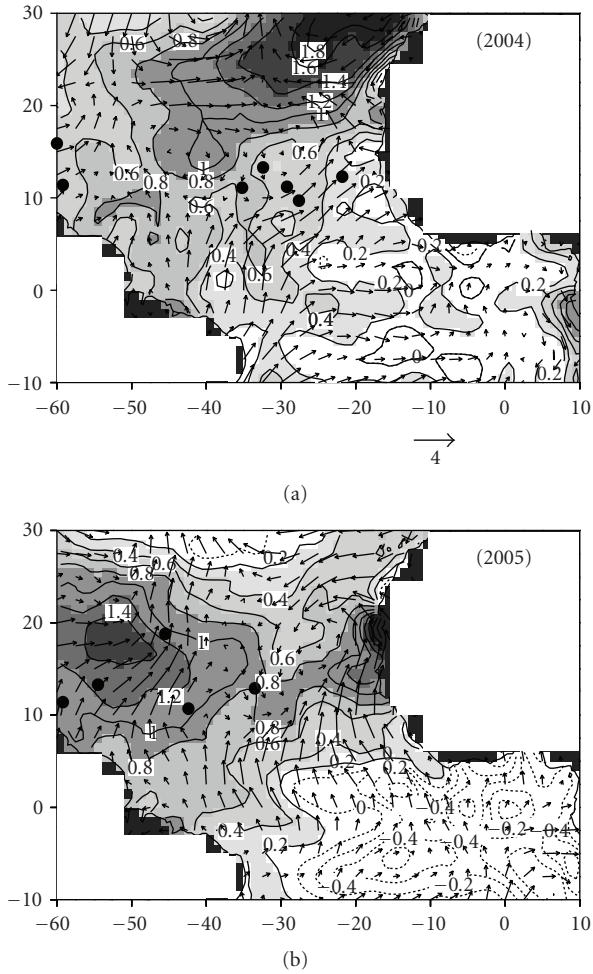

Figure 8: SST anomaly composites (°C) for 2004 (a) and 2005 (b) computed as the averages of the weekly SST anomalies extracted around the periods of the initiation of the long-lived MCSs. Wind anomaly at 1000 hPa from the day of the initiation of the long-lived MCS to the day at which the easterly wave left the African coast is also represented.

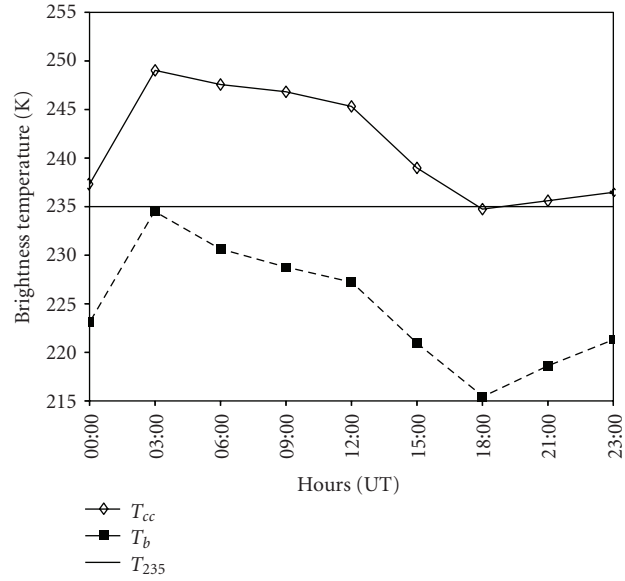

Figure 9: Threshold temperatures used to track the MCSs in the ocean. The continuous curve (T_{cc}) is the dynamic threshold temperature used to define the MCSs, and the dotted curve (T_b) is the dynamic threshold temperature used to define the convective cells merged inside the MCSs. The fixed T_{235} is represented by the horizontal line.

indicate a strengthening of the equatorial upwelling of colder water at this time of the year. Positive and negative SST anomaly cores thus form an anomalous oceanic dipole, similar to the historical dipole studied many times in the past [35]. It is well known that a typical dipole episode is characterized by the simultaneous manifestation of out-of-phase relationship in the tropical Atlantic SST. The north-south anomaly pattern of SST could be simply addressed by the entire anomalous trade wind system [36]. A weaker northeast trades and an enhanced southeast trades affect the thermocline depth along the equator with an abnormal elevation at the eastern side of the tropical basin and an abnormal deepening in the west. These patterns induce warm SST anomalies toward the northern side of the basin, and cold SST anomalies in the equatorial and southern oceanic domains. Such climatic episode favours the establishment of deep convection over the northern Atlantic Ocean, enhances the continental convergence associated with the monsoon that impacts on the West African MCSs formation, and engenders a moister rainy season in West Africa [37, 38]. That process contributes to the intensification of the easterly waves associated with hurricane generation [39]. This influences the static moisture stability [40] and supports an ideal environment for hurricane cyclogenesis.

4. Summary and Conclusion

The objective of this study was to investigate some atmospheric conditions over West Africa a few days before hurricane formation in the tropical North Atlantic. We analyzed the possible coherent relationships between these events and the following variables: easterly waves (through relative vorticity) and the occurrence of precipitation over the West Africa, MCSs which are generated over West Africa and dissipate over the ocean, and oceanic surface conditions. The study examined the periods from June to November in 2004 and 2005.

From the 23 tropical cyclones that produced hurricanes in 2004 (nine events) and 2005 (14 events), we selected 12 H events that were generated (as tropical depressions) close enough to West Africa, that roughly coincided with AEWs over the ocean and with MCSs that crossed westwards the West African coast. Using a diagnostic backward analysis of the date and location of each of the 12 H initiations, it was possible to follow backward the AEWs up to the African continent around 17°W. Then, using an adaptation of the ForTraCC algorithm model to generate the MCS trajectories at 30-minute intervals, we tracked all the lifecycles of the MCSs that formed over the continent and was living around

the moment and place when these AEWs leaved the West African coast. To follow the systems, an innovative threshold temperature, called the "dynamic temperature", was defined and applied to track the convective clusters. Only MCSs whose lifespan were longer than 2.5 hours were examined in this study. Most of the selected MCSs initiated in West Africa around Ivory Coast and dissipated over the ocean or near the African coast.

The AEW trajectories were themselves composed of a large number of MCSs, which initiated and dissipated successively, with different life cycles and durations. The precipitation cores were also related to an occurrence of convective activity indicated by the intermittent presence of the MCSs. Thus, it is hypothesized that the fragmented stratiform clouds that occur during the dissipation phase of the MCSs propagate westward embedded in the easterly wave trajectory. These fragmented stratiform clouds could be the mechanism that triggers new convection by increasing the relative vorticity, contributing to the intensification of the AEWs, and facilitating the development of new convection.

The SST anomaly patterns during the 12 selected Hs in 2004 and 2005 all showed an N–S anomaly dipole, similar to that discussed several times in the past, with abnormal warm conditions in the tropical North Atlantic, and abnormal cold conditions in the Gulf of Guinea associated with an increase in the equatorial seasonal upwelling. The warm condition over the tropical North Atlantic was associated to an abnormal decrease of the Northeast trade wind in the vicinity of West Africa. Therefore, this strengthening in the N–S gradient of SST could also influence the static moisture stability. This result must be verified for other years. The buoys of the Prediction and Research Moored Array in the Tropical Atlantic (PIRATA) [41], which are located in the region, are an excellent facility from which to test and monitor this behaviour.

Appendix

Calculation of the Dynamic Threshold

From the available 2004-2005 MCS dataset over the ocean, an analysis was performed to define the dynamic temperature threshold, which was subsequently used in this study. We first calculated the occurrence probabilities (not shown) of having a cloud top brightness temperature lower than 235 K (hereafter T_{235}). For instance, this probability was 9.0% at 19:00 universal time (UT) and only 4.6% at 16:00 UT. Therefore, a probability of 9% at the time of maximum ocean activity was considered to define the dynamic temperature threshold that allows the tracking of MCSs during a lifetime greater than that of T_{235}, even during suppressed diurnal cycle activity.

All the brightness temperatures of less than 300 K in each image are classified in ascending order. n_t is the number of brightness temperature values lower than 300 K for each image, and $\mathrm{Pb}(0.09) = N/n_t$ is the probability equal to 9% of a brightness temperature (T_{IR}) at the Nth position.

The position N is calculated by

$$N = \mathrm{int}(n_t * 0.09), \tag{A.1}$$

where int is the integer part of the product $n_t * 0.09$.

Finally, the T_{IR} (hereafter T_{CC}) value is calculated at this N position for each image. This technique provides an adaptive brightness threshold temperature for each moment of the day, which allowed each MCS to be followed with the greatest accuracy.

As seen previously, FORTRACC uses two threshold temperatures: one to define the MCS as a whole (T_{CC}), and the other (lower) to define the more intense cells, which can merge inside the MCS. To define a dynamic temperature (T_b) for this colder temperature, the same procedure was applied by considering the probability of a brightness temperature equal to 210 K (this is the usual value used for the coldest threshold).

Figure 9 shows the diurnal evolution of T_{CC} and T_b on the ocean, and of the brightness temperature T_{235} fixed at 235 K. As already observed in previous works [42, 43], the convective activity was higher at the end of the night, in the very early morning. Then, T_{CC} and T_b decreased from 10:00 UT to 18:00 UT, when T_{CC} becomes equal to T_{235}. A comparison of the FORTRACC outputs for the dynamic temperature (T_{CC}) and the outputs for the fixed temperature (T_{235}) indicates consistently more numerous events with a larger cloud cover (higher by factors of 1.3 and 1.4, resp.) and longer MCS trajectories for the T_{CC} case.

Acknowledgments

This work is part of the CNPq-IRD Project "Climate of the Tropical Atlantic and Impacts on the Northeast" (CATIN), no. CNPq Process 492690/2004-9. Y. K. Kouadio. stayed in 2006 at *Centro de Previsão do Tempo e Estudos Climáticos* of the *Instituto Nacional de Pesquisas Espaciais (CPTEC/INPE)* and was supported by Institut de Recherche pour le Développement (IRD) grant (2006-2007).

References

[1] S. B. Goldenberg, C. W. Landsea, A.M. Mestas-Nuñez, and W. M. Gray, "The recent increase in Atlantic hurricane activity: causes and implications," *Science*, vol. 293, no. 5529, pp. 474–479, 2001.

[2] L. J. Shapiro, "The three-dimensional structure of synoptic-scale disturbances over the tropical Atlantic," *Monthly Weather Review*, vol. 114, no. 10, pp. 1876–1891, 1986.

[3] S. B. Goldenberg and L. J. Shapiro, "Physical mechanisms for the association of El Niño and West African rainfall with Atlantic major hurricane activity," *Journal of Climate*, vol. 9, no. 6, pp. 1169–1187, 1996.

[4] R. W. Burpee, "Characteristics of North African easterly waves during the summers of 1968 and 1969," *Journal of the Atmospheric Sciences*, vol. 31, pp. 1556–1570, 1974.

[5] L. A. Avila and R. J. Pash, "Atlantic tropical systems of 1992," *Monthly Weather Review*, vol. 120, pp. 2688–2696, 1992.

[6] L. A. Avila and R. J. Pash, "Atlantic tropical systems of 1993," *Monthly Weather Review*, vol. 123, pp. 887–896, 1995.

[7] C. W. Landsea, "A climatology of intense (or major) Atlantic hurricanes," *Monthly Weather Review*, vol. 121, no. 6, pp. 1703–1713, 1993.

[8] L. A. Avila, "Atlantic tropical systems of 1990," *Monthly Weather Review*, vol. 119, no. 8, pp. 2027–2033, 1991.

[9] J. Molinari, D. Vollaro, S. Skubis, and M. Dickinson, "Origins and mechanisms of eastern pacific tropical cyclogenesis: a case study," *Monthly Weather Review*, vol. 128, no. 1, pp. 125–139, 2000.

[10] S. W. Payne and M. M. McGarry, "The relationship of satellite inferred convective activity to easterly waves over West Africa and the adjacent ocean during phase III of GATE," *Monthly Weather Review*, vol. 105, pp. 413–420, 1977.

[11] W. R. Cotton and R. A. Anthes, *Storm and Cloud Dynamics*, Academic Press—Harcourt Brace Jovanovich, New York, NY, USA, 1989.

[12] D. L. Bartels and R. A. Maddox, "Midlevel cyclonic vortices generated by mesoscale convective systems," *Monthly Weather Review*, vol. 119, no. 1, pp. 104–118, 1991.

[13] M. Saïdou and H. Sauvageot, "Cyclogenesis off the African Coast: the case of cindy in August 1999," *Monthly Weather Review*, vol. 133, no. 9, pp. 2803–2813, 2005.

[14] C. W. Landsea and W. M. Gray, "The strong association between western Sahelian monsoon rainfall and intense Atlantic hurricanes," *Monthly Weather Review*, vol. 5, pp. 435–453, 1992.

[15] R. H. Simpson, "The hurricane disaster potential scale," *Weatherwise*, vol. 27, pp. 169–186, 1974.

[16] R. A. Houze Jr., "Structure and dynamics of a tropical squall-line system," *Monthly Weather Review*, vol. 105, pp. 1540–1567, 1977.

[17] I. Velasco and J. M. Fritsch, "Mesoscale convective complexes in the Americas," *Journal of Geophysical Research*, vol. 92, no. 8, pp. 9591–9613, 1987.

[18] L. A. T. Machado and W. B. Rossow, "Structural characteristics and radiative properties of tropical cloud clusters," *Monthly Weather Review*, vol. 121, pp. 3234–3260, 1993.

[19] V. Mathon, H. Laurent, and T. Lebel, "Mesoscale convective system rainfall in the Sahel," *Journal of Applied Meteorology*, vol. 41, no. 11, pp. 1081–1092, 2002.

[20] V. Mathon, A. Diedhiou, and H. Laurent, "Relationship between easterly waves and mesoscale convective systems over the Sahel," *Geophysical Research Letters*, vol. 29, no. 8, 1216 pages, 2002.

[21] H. Laurent, L. A. T. Machado, C. A. Morales, and L. Durieux, "Characteristics of the Amazonian mesoscale convective systems observed from satellite and radar during the WETAMC/LBA experiment," *Journal of Geophysical Research D*, vol. 107, no. 20, pp. LBA 21.1–LBA 21.17, 2002.

[22] E. Kalnay, M. Kanamitsu, R. Kistler, et al., "The NCEP/NCAR 40-year reanalysis project," *Bulletin of the American Meteorological Society*, vol. 77, no. 3, pp. 437–471, 1996.

[23] G. J. Huffman, R. F. Adler, M. M. Morrissey, D. T. Bolvin, et al., "Global precipitation at one-degree daily resolution from multisatellite observations," *Journal of Hydrometeorology*, vol. 2, no. 1, pp. 36–50, 2001.

[24] R. W. Reynolds, N. A. Rayner, T. M. Smith, D. C. Stokes, and W. Wang, "An improved in situ and satellite SST analysis for climate," *Journal of Climate*, vol. 15, no. 13, pp. 1609–1625, 2002.

[25] D. A. Vila, L. A. T. Machado, H. Laurent, and I. Velasco, "Forecast and tracking the evolution of cloud clusters (ForTraCC) using satellite infrared imagery: methodology and validation," *Weather and Forecasting*, vol. 23, no. 2, pp. 233–245, 2008.

[26] L. A. T. Machado, J.-P. Duvel, and M. Desbois, "Diurnal variations and modulation by easterly waves of the size distribution of convective cloud clusters over West Africa and the Atlantic Ocean," *Monthly Weather Review*, vol. 121, no. 1, pp. 37–49, 1993.

[27] L. A. T. Machado, W. B. Rossow, R. L. Guedes, and A. W. Walker, "Life cycle variations of mesoscale convective systems over the Americas," *Monthly Weather Review*, vol. 126, no. 6, pp. 1630–1654, 1998.

[28] V. Mathon and H. Laurent, "Life cycle of Sahelian mesoscale convective cloud systems," *Quarterly Journal of the Royal Meteorological Society*, vol. 127, no. 572, pp. 377–406, 2001.

[29] L. A. T. Machado and H. Laurent, "The convective system area expansion over Amazonia and its relationships with convective system life duration and high-level wind divergence," *Monthly Weather Review*, vol. 132, no. 3, pp. 714–725, 2004.

[30] C. Morel and S. Senesi, "A climatology of mesoscale convective systems over Europe using satellite infrared imagery. I: methodology," *Quarterly Journal of the Royal Meteorological Society*, vol. 128, no. 584, pp. 1953–1972, 2002.

[31] G. J. Berry and C. Thorncroft, "Case study of an intense African easterly wave," *Monthly Weather Review*, vol. 133, no. 4, pp. 752–766, 2005.

[32] N. L. Frank, "Atlantic tropical systems of 1974," *Monthly Weather Review*, vol. 103, pp. 294–300, 1975.

[33] M. Ćurić, D. Janc, and V. Vučković, "The influence of merging and individual storm splitting on mesoscale convective system formation," *Atmospheric Research*, vol. 93, no. 1–3, pp. 21–29, 2009.

[34] R. A. Houze Jr., "Mesoscale convective systems," *Reviews of Geophysics*, vol. 42, no. 4, Article ID RG4003, 2004.

[35] J. Servain, "Simple climatic indices for the tropical Atlantic Ocean and some applications," *Journal of Geophysical Research*, vol. 96, no. 8, pp. 15137–15146, 1991.

[36] J. Servain, I. Wainer, H. L. Ayina, and H. Roquet, "The relationship between the simulated climatic variability modes of the tropical Atlantic," *International Journal of Climatology*, vol. 20, no. 9, pp. 939–953, 2000.

[37] E. K. Vizy and K. H. Cook, "Development and application of a mesoscale climate model for the tropics: influence of sea surface temperature anomalies on the West African monsoon," *Journal of Geophysical Research D*, vol. 107, no. 3, Article ID 4023, 2002.

[38] B. Sultan, S. Janicot, and A. Diedhiou, "The West African monsoon dynamics. Part I: documentation of intraseasonal variability," *Journal of Climate*, vol. 16, no. 21, pp. 3389–3406, 2003.

[39] W. M. Gray, C. W. Landsea, P. W. Mielke Jr., and K. J. Berry, "Predicting Atlantic basin seasonal tropical cyclone activity by 1 August," *Weather & Forecasting*, vol. 8, no. 1, pp. 73–86, 1993.

[40] J. S. Malkus and H. Riehl, "On the dynamics and energy transformations in steady-state hurricanes," *Tellus*, vol. 12, pp. 1–20, 1960.

[41] B. Bourlès, R. Lumpkin, M. J. McPhaden, et al., "The PIRATA program: history, accomplishments, and future directions," *Bulletin of the American Meteorological Society*, vol. 89, no. 8, pp. 1111–1125, 2008.

[42] S. S. Chen and R. A. Houze Jr., "Diurnal variation and lifecycle of deep convective systems over the tropical Pacific warm

pool," *Quarterly Journal of the Royal Meteorological Society*, vol. 123, pp. 357–388, 1997.

[43] T. J. Hall and T. H. Yonder Haar, "The diurnal cycle of west pacific deep convection and its relation to the spatial and temporal variation of tropical MCSs," *Journal of the Atmospheric Sciences*, vol. 56, no. 19, pp. 3401–3415, 1999.